

Reactive magnetron sputtered ZrCN decorative films for plastic substrates

Michael Brazil

Vergason Technology, Inc. Van Etten, NY

Abstract

With a range of possible colors, cathodic arc ZrCN PVD coatings have been used as durable decorative coatings on metals for years. We present results for ZrCN from a magnetron sputtering system without substrate bias, and staying within the thermal limits of a plastic substrate. The relationships between color and abrasion resistance are discussed, particularly for dark reflection levels.

Introduction

In the market for shiny, eye-catching finishes, there is a persistent desire for a dark, high gloss look. When paints are insufficient for the performance, PVD coatings have been historically available. Some applications require metal substrates, for example automobile wheels. In many applications, the mechanical properties of plastic are sufficient. Electroplating has long been available for many such applications. It is common for plumbing fixtures to begin with an electroplated surface to which a PVD decorative layer is applied. That process requires plating grade plastics, either acrylonitrile butadiene styrene (ABS) or polycarbonate/ABS blends. Although unnecessary for PVD, the electroplated base requires a butadiene etch to provide an anchoring texture. This selection of plastic creates a temperature limit, since they soften in the range of 95°C to 130°C.

The defined appearance has to be durable. By “dark”, a common definition would be CIELAB D65 values near (40, 0, 0). While gloss value should be specified for the product, a hard PVD coating is likely to be highly specular and relatively thin compared to the substrate texture. Product gloss will be determined by the substrate. The coating must adhere well and appear unchanged after exposure to ultraviolet light, immersion in harsh cleaners, immersion in corrosive chemicals, thermal shock, and abrasion. Abrasion resistance of coatings intended for plumbing fixtures was assessed by cycling steel wool soap pads, e.g. Brillo[®] or Ako[®] pads, 1000 strokes under 20 N/cm² (29 psi) load.

Transition metal nitrides and carbonitrides of deposited films have been extensively used in industrial applications. Zirconium is an attractive transition metal due to its outstanding chemical and physical properties. Research has shown that ZrN has a high thermal [1] and chemical stability [2], as well as high hardness [3] and low electrical resistivity [4]. ZrN films have been used for decorative purposes due to their golden color [3], as well as other colors [5]. Carbonitrides can be dark rather than gold. ZrCN films have demonstrated high hardness [21], high chemical and thermal stability [6], good

tribological and corrosion behavior [3], and are therefore good candidates for effective protective coatings against wear, abrasion and corrosion [7].

ZrCN coatings have been prepared by different techniques including plasma assisted CVD [8], arc evaporation [9,10], magnetron sputtering [13] and ion beam sputtering [14]. Literature concerning ZrCN films deals with the process details of plasma-aided chemical vapor deposition, mainly discussing how to grow ZrCN films at relatively low temperature [8,11]. Hollstein et al. [9] deposited a group of ZrCN films by means of cathodic arc and investigated their use as tools for minimally invasive surgery. The result indicated that ZrCN is a candidate for layers on surgical tools where short-term biocompatibility is required. Rie et al. [12] deposited a group of Zr-based films and found good corrosive resistance of the ZrCN films. Yao et. al. [13] showed that over a C₂H₂:N₂ ratio of 4 to 2, the hardness and wear behavior of ZrCN films depended strongly on the ratio, with highest hardness and least wear at the lowest ratio of C₂H₂/N₂ reactive gas flow rates. Methane flow reveals a maximum in hardness, corresponding to a theoretical model [14].

Direct current reactive magnetron sputtering offers a few potential advantages over a cathodic arc approach to ZrCN on plastic parts. Many molded parts have complex, high aspect ratio geometry. To achieve uniform coating on the visible areas, it is necessary to move parts through many angles and positions. This is usually done with either a single axis or planetary rotation arrangement. The plastic is also electrically insulating, unless electroplated. Cathodic arc coatings typically rely on an electrical bias for density and hardness. The motion and insulating nature of substrates can make applying a bias challenging in a production environment. A sputtered coating may not need bias. A sputtered film is also likely to be smoother, without the macro particles common to cathodic arc. Even if the properties of the sputtered film were on par with cathodic arc film, the large installed base of sputter tools would benefit from adding such a coating to their repertoire.

The bounds on film thickness are set by heat tolerance of the substrate and absorptivity of the coating. Substrate heating mechanisms for sputtered films have been well documented [15,16]. The need to stop deposition before the substrate is softened sets an upper limit. Although a large gamut of colors is possible if interference effects are employed [17], a uniform color from PVD on parts of arbitrary 3D shapes can be challenging. Typically, minor variations in film thickness produces undesired rainbow effects. One way to obtain uniformity is to use a combination of thickness and absorptivity

that keeps the amount of reflection from the coating-substrate interface that arrives at the air-coating interface less than a few percent of the reflection from the air-coating interface. This product of absorptivity and thickness sets a lower limit on thickness.

Methods and Results

Development began with locating a suitable ZrN process. With a 50/50 mix of Ar and N₂, a flow was found where the target was fully poisoned. This produced the well-known gold color. From there, acetylene (C₂H₂) was added. It was found that the resulting film was not only very hard, but also very electrically insulating. After producing a few films using the chamber as anode, the disappearing anode effect was overcome with a water-cooled discrete anode and an Advanced Energy AMS/DMS operated in what has been referred to as “Pelley mode.” [18]

A series of coatings was produced with total gas flow between 400 sccm and 600 sccm. Relative flow rates of the three process gases are shown in Table 1.

Although many approaches to determining the absorption coefficients of thin films have been addressed over the decades [19] using spectrophotometers or ellipsometers, a rapid and inexpensive method was used that was sufficient to guide process refinements. Films thin enough to allow low transmission across the visible spectrum were deposited onto glass slides. Transmission and film-side reflection were measured with an Ocean Optics USB2000 spectrometer. With d as thickness, using the relations

$$A(\lambda) = 1 - T(\lambda) - R(\lambda)$$

$$A(\lambda) = e^{-\alpha(\lambda)d}$$

plots of absorptivity, α , were produced, as in Figure 1. We found we could ignore errors in derivation of α from sources such as back side reflection and mis-registration between T and R measurement locations for the purpose of guiding pro-

Table 1. Process parameters and absorptivity at 550 nm for ZrCN. Total gas flows ranged from 400 sccm to 600 sccm.

Run	Ar	N ₂	C ₂ H ₂	Power (W-cm ⁻²)	anode	a_{550} mm ⁻¹
A	54%	45%	2%	19	chamber	1.37
B	53%	44%	3%	19	chamber	0.91
C	51%	43%	6%	19	chamber	1.09
D	47%	39%	14%	19	chamber	1.19
E	40%	59%	2%	19	chamber	0.37
F	42%	22%	36%	12	discrete	2.6
G	42%	22%	36%	12	discrete	3.11
H	49%	17%	34%	12	discrete	2.74
K	49%	17%	34%	14	discrete	3.88

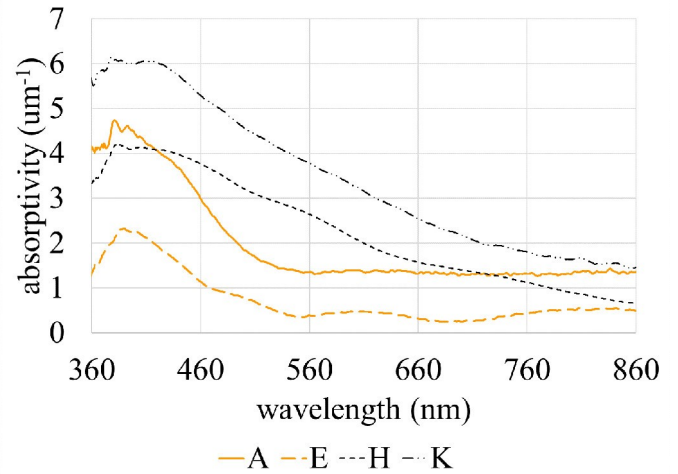


Figure 1. Absorptivity spectra of 4 ZrCN films.

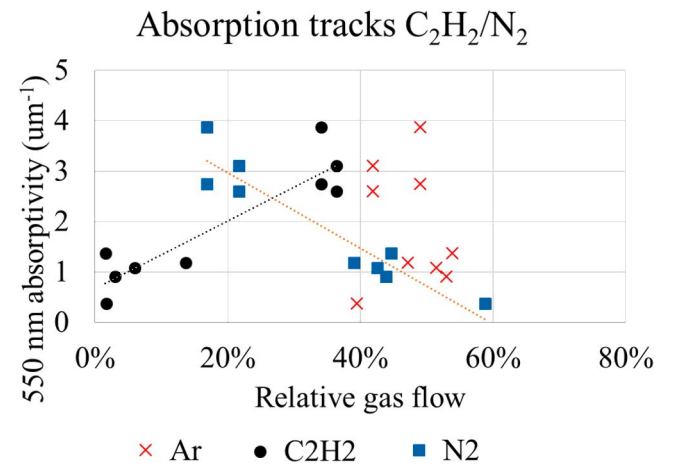


Figure 2. Absorptivity at 550 nm as a function of relative gas flows.

cess parameters. Optical thin film modeling would have required more accurate, traditional methods. Figure 1 shows the spectra of four different films. The lower plots are from films with 15% or less of C₂H₂, while the upper plots are from films with 33% or more C₂H₂. The low C₂H₂ films had a gold appearance, although the color was not as saturated as ZrN films. The change in shape of the plots indicates a fundamental change in the material band structure. Table 1 shows the values for each coating at 550 nm. Figure 2 shows that, while absorptivity does not depend exclusively on C₂H₂, it does depend strongly and, to first order, linearly.

A subsequent series of coatings that were thick enough to be opaque were produced on both plastic and silicon wafer substrates. Many of these films displayed high compressive stress; some films spontaneously delaminated. Stress was measured using precharacterized Si(100) wafers, a profilometer to measure curvature, and Stoney’s equation [20]. Figure 3 shows stresses measured on silicon wafers as compressive as -800 MPa. However, on plastic substrates, the film stress is likely to be much more compressive. The stress due to thermal

contraction is likely significant, and can be estimated. The coating is deposited hot, and the entire system contracts as it cools to room temperature. The total stress on the film is comprised of the thermal stress, the intrinsic film stress, and any externally applied forces.

$$\sigma_{total} = \sigma_{thermal} + \sigma_{intrinsic} + \sigma_{extrinsic}$$

The film is much thinner than either of the substrates. Assuming the mechanical properties are isotropic in the plane of the coating, and that the coefficient of thermal expansion, γ , does not vary much over the temperature range,

$$\sigma_{thermal} = \frac{E_f}{(1-\nu_f)} (\gamma_f - \gamma_s) (T_{dep} - T_{ambient})$$

If external forces are negligible, or identical to both the wafer and plastic,

$$\sigma_{total}^{wafer} = \sigma_{thermal}^{wafer} + \sigma_{intrinsic}^{film}$$

$$\sigma_{total}^{plastic} = \sigma_{thermal}^{plastic} + \sigma_{intrinsic}^{film}$$

The total stress on the wafer is what is measured by the profilometer. When these are subtracted,

$$\sigma_{total}^{wafer} - \sigma_{total}^{plastic} = (\sigma_{thermal}^{wafer} - \sigma_{thermal}^{plastic})$$

$$\sigma_{thermal}^{wafer} - \sigma_{thermal}^{plastic} = \frac{E_f}{(1-\nu_f)} (\gamma_{plastic} - \gamma_{wafer}) (T_{dep} - T_{amb})$$

The γ of the film disappears from the relationship. Using values from Table 2, the film on plastic may be -3.1 GPa more compressive than the measured value. This analysis may over-estimate the thermal effect, since it assumes the system was at thermal equilibrium before any coating was applied, and that the different substrates absorb heat equally. However, it shows that the thermal effect cannot be ignored.

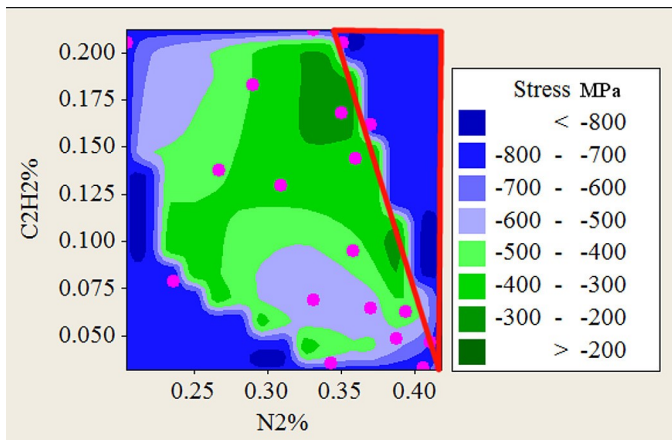


Figure 3. Contour plot showing compressive stress dependence on relative flow of gases. Pink circles indicate values where data was collected. Red outline denotes area particularly to be avoided.

Table 2. Nominal values of materials in thermal stress calculation.

Parameter	Nominal value
E_f	400 GPa
ν_f	0.25
γ Covestro T65XF®	$80 \times 10^{-6}/^\circ\text{K}$
γ Si (100)	$2.6 \times 10^{-6}/^\circ\text{K}$
T_{dep}	100°C
T_{amb}	25°C

Abrasion was assessed as the percentage of area where coating was removed. High percentage removal was observed from films made with very high C_2H_2 flows. Films that required microscopic observation to assess steel wool abrasion were assessed between 0% and 2% removal. Among these, Figure 4

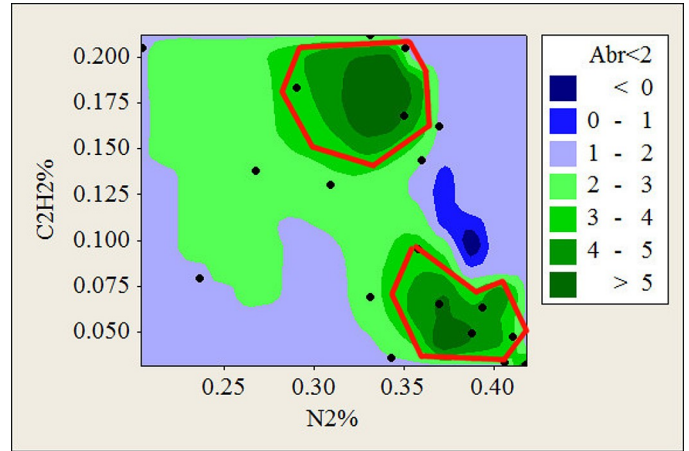


Figure 4. Contour plot of abrasion damage as a function of reactive gas flows. Rank of 0 means no damage was observed. Black dots represent conditions where films were produced. Only samples with very low damage are included. Red outline denotes area particularly to be avoided.

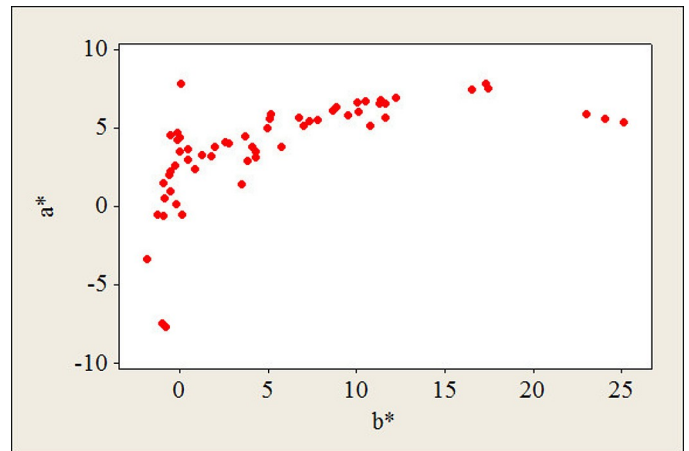


Figure 5. Chromaticity of ZrCN films produced with $0.08 < \text{C}_2\text{H}_2/\text{N}_2 < 1$.

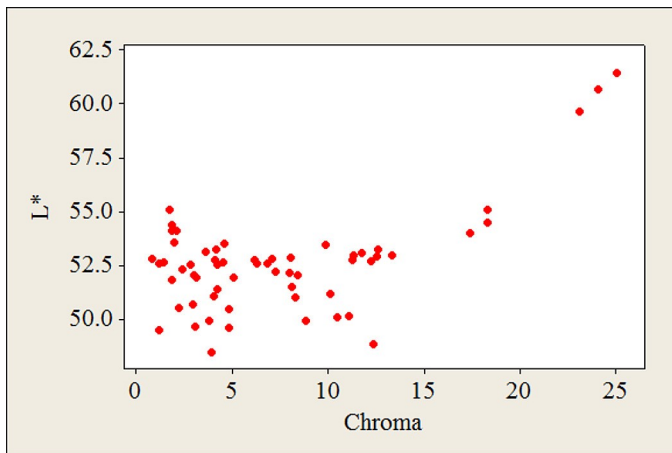


Figure 6. L^* as a function of chroma.

shows that flows in the vicinity of 10% C_2H_2 and 38% N_2 survived without damage.

Although the opaque ZrCN films displayed a wide range of colors, those colors followed a pattern. Figure 5 shows that the films followed a characteristic track for coatings produced with reactive gas ratios C_2H_2/N_2 between 0.08 and 1. Consider chromaticity, C^* , defined as

$$C^* = \sqrt{a^* + b^*}$$

in the (L^* , a^* , b^*) system. Figure 6 shows that the films with lower chromaticity were also darker. Figure 7 shows that low chromaticity was achieved at higher values of both reactive gases.

Discussion

The competing demands of good abrasion resistance, moderate stress for good adhesion, and dark, neutral color are almost mutually exclusive. Figure 8 overlays the regions best avoided due the various criteria on the reactive gas space, revealing a small process window that promises the best film.

In the future, methods of creating greater incorporation of carbon are needed to make a darker coating without overheating the plastic substrate or losing abrasion resistance. This may

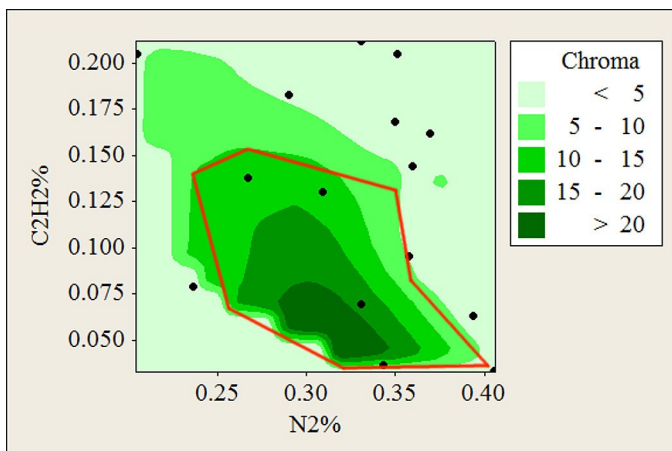


Figure 7. Chroma as a function of reactive gas flow ratios. Red outline denotes area particularly to be avoided.

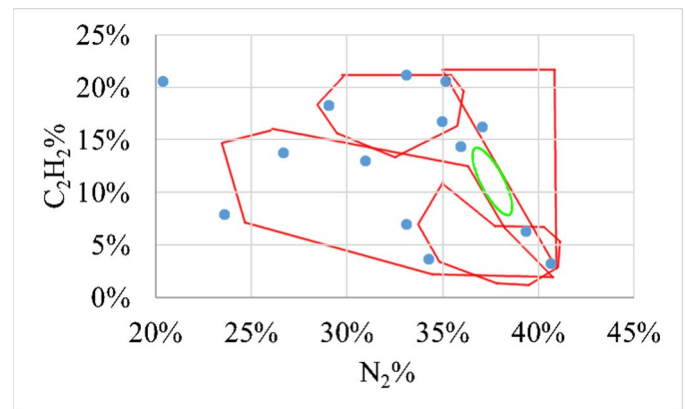


Figure 8. Overlay of areas to avoid reveals promising region around 37% N_2 , 12% C_2H_2 .

include addition of a.c. or r.f. electrodes contemporary with the sputtering process. The sputtering process space for both hard and dark films may be opened by operating at less than fully poisoned under emission spectrometry control. This would change the relative arrival rate ratio of metal/non-metal which has been shown to alter film hardness [21].

Conclusions

Direct current reactive magnetron sputtering with a discrete anode can produce moderately dark, neutral ZrCN coatings on plastic parts in a very narrow process space.

Acknowledgments

Many thanks to Vergason Technology, and to Gary Vergason, Mark Fitch and Rick Smith for their continued support.

References

- [1] D. Wu, Z. Zhang, W. Fu, X. Fan, H. Guo, "Structure, electrical and chemical properties of zirconium nitride films deposited by dc reactive magnetron sputtering," *Appl. Phys. A* 64, pp. 593-595, 1997. <http://dx.doi.org/10.1007/s003390050522>
- [2] E. Kelesoglu, C. Mitterer, M.K. Kazmanli, M. Urgan, "Corrosion characteristics of plain carbon steel coated with TiN and ZrN under high-flux ion bombardment," *Surf. Coat. Technol.*, 116, pp. 82-86, 2002. [http://dx.doi.org/10.1016/S0257-8972\(02\)00358-4](http://dx.doi.org/10.1016/S0257-8972(02)00358-4)
- [3] R. Constantin, B. Miremad, "Performance of hard coatings, made by balanced and unbalanced magnetron sputtering, for decorative applications," *Surf. Coat. Technol.*, 120-121, pp. 728-733, 1999. [http://dx.doi.org/10.1016/S0257-8972\(99\)00366-7](http://dx.doi.org/10.1016/S0257-8972(99)00366-7)
- [4] C.C. Wang, S.A. Akbar, W. Chen, V.D. Patton, "Electrical properties of high-temperature oxides, borides, carbides, and nitrides," *J. Mater. Sci.*, 30, pp. 1627

- 1641, 1995. <http://dx.doi.org/10.1007/BF00351591>
- [5] M.H. Bouix and C.P. Dumortier, "Color Trends in PVD," *43rd Annual Technical Conference Proceedings of the Society of Vacuum Coaters*, pp. 52-54, 2000.
- [6] W. Fleischer, T. Trinh and P. Willich, "Surface Oxidation of Decorative Hard Coatings with Enriched Carbon Content," *43rd Annual Technical Conference Proceedings of the Society of Vacuum Coaters*, pp. 46-51, 2000.
- [7] M. Braica, V. Braica, M. Balaceanu, C.N. Zoitaa, A. Kissa, A. Vladescu, A. Popescub, R. Ripeanub, "Structure and properties of Zr/ZrCN coatings deposited by cathodic arc method," *Materials Chemistry and Physics* 126, pp. 818-825, 2011. <http://dx.doi.org/10.1016/j.matchemphys.2010.12.036>
- [8] L. Alberts, D. Boscarino, A. Patelli, V. Rigato, H. Ahn, and K.T. Rie, "Ion beam analysis of low-temperature MO-PACVD coatings," *Surf. Coat. Tech.*, 169-170, pp. 388-392, 2003. [http://dx.doi.org/10.1016/S0257-8972\(03\)00062-8](http://dx.doi.org/10.1016/S0257-8972(03)00062-8)
- [9] F. Hollstein, D. Kitta, P. Louda, F. Pacal, J. Meinhardt, "Investigation of low-reflective ZrCN PVD-arc coatings for application on medical tools for minimally invasive surgery," *Surf. Coat. Technol.* 142-144, pp. 1063, 2001. [http://dx.doi.org/10.1016/S0257-8972\(01\)01222-1](http://dx.doi.org/10.1016/S0257-8972(01)01222-1)
- [10] J.-D. Gu, P.-J. Chen, "Investigation of the corrosion resistance of ZrCN hard coatings fabricated by advanced controlled arc plasma deposition," *Surf. Coat. Technol.* 200, pp. 3341-3346, 2006. <http://dx.doi.org/10.1016/j.surfcoat.2005.07.049>
- [11] J. Wöhle, C. Pfohl, K.-T. Rie, A. Gebauer-Teichmann, S.K. Kim, "Deposition of TiCN and ZrCN layers on light metals by PACVD method using radio frequency and pulsed-DC plasma," *Surf. Coat. Technol.* 131, pp. 127-130, 2000. [http://dx.doi.org/10.1016/S0257-8972\(00\)00749-0](http://dx.doi.org/10.1016/S0257-8972(00)00749-0)
- [12] K.-T. Rie, A. Gebauer, J. Wöhle, "Plasma assisted CVD for low temperature coatings and corrosion resistance," *Surf. Coat. Technol.* 86-87, pp. 498-506, 1996. [http://dx.doi.org/10.1016/S0257-8972\(96\)03177-5](http://dx.doi.org/10.1016/S0257-8972(96)03177-5)
- [13] S.H. Yao, Y.L. Su, W.H. Kao, K.W. Cheng, "Wear behavior of DC unbalanced magnetron sputter deposited ZrCN films," *Materials Letters* 59, pp. 3230 - 3233, 2005. <http://dx.doi.org/10.1016/j.matlet.2005.04.064>
- [14] M.M. Larijani, M.B. Zanjanbarb, A. Majdabadia, "The effect of carbon fraction in Zr(C, N) films on the nano-structural properties and hardness," *J. Alloys and Compounds* 492, pp. 735-738, 2010. <http://dx.doi.org/10.1016/j.jallcom.2009.12.035>
- [15] R.P. Howson. and H.A. J'Afer, "Substrate effects from an unbalanced magnetron," *Thin Solid Films* 193-194, p. 127-137, 1990. [http://dx.doi.org/10.1016/S0040-6090\(05\)80020-3](http://dx.doi.org/10.1016/S0040-6090(05)80020-3)
- [16] W.D. Westwood, *Sputter Deposition*, American Vacuum Society, 2003, pp. 64-66.
- [17] M. Eerden, M. Schreurs, P. Schreurs, and R. Tieterna, "Oxygen as a Reactive Gas: Opportunities in the Decorative Coating Field," *47th Annual Technical Conference Proceedings of the Society of Vacuum Coaters*, pp. 556-559, 2004.
- [18] D. R. Pellemounter, "Raising the bar on reactive deposition sputter rates," *58th Annual Technical Conference Proceedings of the Society of Vacuum Coaters*, pp. 1-5, 2015.
- [19] Computer software, e.g., "The Essential Macleod," Thin Film Center, Tucson, Arizona; "OptiChar," www.optilayer.com.
- [20] G.C.A.M. Janssen, M.M. Abdalla, F. van Keulen, B.R. Pajuda, and B. van Venrooy, "Celebrating the 100th anniversary of the Stoney equation for film stress: Developments from polycrystalline steel strips to single crystal silicon wafers," *Thin Solid Films* 517, pp. 1858-1867, 2009. <http://dx.doi.org/10.1016/j.tsf.2008.07.014>
- [21] M. Braic, M. Balaceanu, A. Vladescu, C.N. Zoita, V. Braic, "Study of (Zr,Ti)CN, (Zr,Hf)CN and (Xr,Nb)CN films prepared by reactive magnetron sputtering," *Thin Solid Films* 519, pp. 4092-4096, 2011. <http://dx.doi.org/10.1016/j.tsf.2011.01.375>